Climatic Variations on Mars
2. Evolution of Carbon Dioxide Atmosphere and Polar Caps

WILLIAM R. WARD,[1] BRUCE C. MURRAY, AND MICHAEL C. MALIN

Division of Geological and Planetary Sciences, California Institute of Technology, Pasadena, California 91109

The long-term variations in the atmospheric pressure and the polar cap temperature of Mars resulting from the obliquity oscillations (presented by W. R. Ward, 1974) are discussed. In performing these calculations, the assumption is made that the atmosphere is in equilibrium with perennial CO_2 ice deposits at the north pole, as is proposed by R. B. Leighton and B. C. Murray (1966). If heat transport by the atmosphere is neglected, the temperature of CO_2 ice at the poles ranges from ~130°K to ~160°K, the corresponding atmospheric pressure rising from a few tenths of a millibar to ~30 mbar, respectively. The neglect of atmospheric heat transport probably underestimates the peak pressure. Because the altitude of the south cap is ~2 km higher than that of the north cap, CO_2 ice is unstable there and will migrate to the north cap at a rate ~10 g/cm² yr, the implication being that the south residual cap is water ice. A simplified model of the annual polar caps and pressure fluctuations is also presented. This indicates that when the obliquity is at its maximum, the annual caps may be greatly enlarged in both mass and maximum coverage. The modifications introduced by including significant atmospheric heat transport are then discussed. Finally, the implications of different past climatic conditions on the mechanism of eolian erosion are briefly considered.

In a number of earlier papers [*Murray et al.*, 1973; *Ward*, 1973; *Ward*, 1974, designated as paper 1] it was shown that large previously unrecognized periodic changes in the obliquity and orbital eccentricity of Mars were responsible for correspondingly important variations in the global distribution and seasonal intensity of the solar insolation. This paper will address the question of the response of the CO_2 atmosphere and polar caps of Mars to these variations. This work is particularly timely in light of the recent discoveries by Mariner 9 of many puzzling features on the surface of Mars [e.g., *Murray et al.*, 1972; *Soderblom et al.*, 1973; *McCauley et al.*, 1972]. The formation of such structures as the channels, canyon lands, and layered terrain may reflect considerably different conditions in the past. It is therefore of paramount importance to have some idea of the climatic history of Mars.

A complete modeling of the past atmosphere and climate of Mars would include, in addition to insolation variations, such details as atmospheric heat transport [*Leovy and Mintz*, 1969; *Gierasch and Sagan*, 1971; *Gierasch and Toon*, 1973], heat conductivity of the ground [*Leighton and Murray*, 1966; *Cuzzi and Muhleman*, 1972], topographical effects [*Gierasch and Sagan*, 1971; *Blumsack*, 1971; *Blasius*, 1973], and CO_2 gas adsorption by the regolith [*Fanale and Cannon*, 1971]. Such a project is beyond the scope of the present paper, and the quantitative significance of some of these processes is currently the topic of some debate. Instead, an idealized model based largely on the 1966 work of Leighton and Murray is employed. The basic tenet of this model is that the CO_2 atmosphere is in equilibrium with perennial CO_2 ice deposits at the north pole, so that the mean pressure is determined by the average annual polar insolation. Both the long-term behavior and the annual behavior of the model solely as a result of insolation variations are easily ascertained. The most critical omission is probably the heat transport by the atmosphere. Because of this omission the model tends to underestimate the pressure at periods of high annual polar insolation. In a sense these calculations represent a minimum response model. Nevertheless, we expect most of the features of the solutions presented here to be indicative of trends in the history of the climate of Mars. Many of the features are quite interesting, such as the prediction of large changes in the mean atmospheric pressure and polar cap temperatures, a great enlargement of the annual polar caps during periods of high obliquity, and intervals of more intense eolian erosion.

We first look at the long-term behavior of the atmosphere and the polar caps. Occasionally, equations will be employed that are derived in Appendix 1, where a simplified version of the atmosphere–polar cap equilibrium problem that can be solved analytically is presented. This section is followed by a treatment of the annual atmospheric fluctuations and the deposition and evaporation of the annual caps for different past climatic epochs. Some of the modifications introduced by including an atmospheric heat transport term are then indicated. These are in turn followed by a rediscussion of the wind-blown dust models of *Ryan* [1964] and *Sagan and Pollack* [1967, 1969].

Long-Term Behavior

On time scales much longer than an orbital period it is the obliquity θ of Mars rather than the eccentricity e that exerts the most influence on the climate. The reason is that the total annual insolation at the poles of the planet is proportional to the first power of the obliquity, whereas the dependence on the eccentricity is through a second-order term; i.e.,

$$\langle I_p \rangle = (S/\pi)(1 - e^2)^{-1/2} \sin \theta \qquad (1)$$

where $S = 6 \times 10^5$ erg/cm² s is the solar constant at the semimajor axis (1.52 AU) of Mars. The current value of $\langle I_p \rangle$ is 7.8×10^4 erg/cm² s. However, the combined actions of solar and planetary perturbations on the spin axis and the orbit of Mars produce oscillations in the obliquity of the form

$$\theta = \Theta^* - \sum_i N_i \sin (s_i' t + \alpha t \cos \Theta + \gamma_i) \qquad (2)$$

where Θ^* is a constant equal to ~25.2°, $\alpha \cos \Theta$ is the precession frequency of the Mars spin axis, and N_j, s_j', and γ_j are

[1] Present address: Center for Astrophysics, Harvard College Observatory, Cambridge, Massachusetts 02138.

amplitudes, eigenfrequencies, and phase constants, the values of which were given in paper 1. Figure 1 shows the orbital inclination and the obliquity for the past 5×10^6 yr. The value of $\langle I_p \rangle$ varies by over a factor of 2 between the obliquity extremes.

In 1966 Leighton and Murray suggested that the atmosphere of Mars could be in equilibrium with perennial CO_2 ice deposits at the poles. At the crux of the hypothesis is the suggestive coincidence between the observed atmospheric pressure of about 6 mbar and the vapor pressure of CO_2 ice at a temperature T such that the radiation rate equals the average rate of solar energy absorption. In Appendix 1 we present a model calculation that indicates that the average pressure p is determined by an equation of the following type (A9):

$$dp/dt \cong [ag/2\pi R^2 L][(1 - A)\langle I_p \rangle - E\sigma T^4] \quad (3)$$

where $g = 3.8 \times 10^2$ cm/s^2 is the surface acceleration of gravity, $R = 3.4 \times 10^3$ km is the radius of Mars, a is the area of the polar cap, $L = 4.5 \times 10^9$ erg/gm is the latent heat of solid CO_2, $A \approx 0.70$ is the model albedo of the polar cap, and $E \approx 0.85$ and $\sigma = 5.6 \times 10^{-5}$ erg cm^{-2} s^{-1} deg^{-4} are the emissivity and the Stefan-Boltzmann constant, respectively. The atmospheric pressure and the polar cap temperature are related through the vapor pressure curve

$$p = Be^{-T^*/T} \quad (4)$$

with $B = 10^{10.083}$ mbar and $T^* = 3148$°K [*Washburn*, 1928]. For small changes in p and T, (1)-(4) can be combined to yield

$$\frac{d}{dt}\Delta p + \frac{\Delta p}{\tau} = -\tfrac{1}{4}p_0 \frac{T^*}{T_0}\frac{\cot \Theta^*}{\tau} \cdot \sum_i N_i \sin (s_i' t + \alpha t \cos \Theta + \gamma_i) \quad (5)$$

which is easily integrated; i.e.,

$$\Delta p = -\tfrac{1}{4}p_0 \frac{T^*}{T_0}\frac{\cot \Theta^*}{\tau} \cdot \sum_i N_i[(s_i' + \alpha \cos \Theta)^2 + \tau^{-2}]^{-1} \times \{\tau^{-1} \sin [(s_i' + \alpha \cos \Theta)t + \gamma_i] - (s_i' + \alpha \cos \Theta) \cos [(s_i' + \alpha \cos \Theta)t + \gamma_i]\} \quad (6)$$

where the characteristic response time of the system is

$$\tau = \pi R^2 L p_0 T^*/2agT_0(1 - A)\langle I_p^* \rangle \quad (7)$$

(The increments Δp and ΔT are measured with respect to values p_0 and T_0 when $\theta = \Theta^*$.)

We should say a word about the appropriate value of the cap area a to be used in (7). In Appendix 1, where the latitudinal variation in insolation is neglected, the area of the perennial cap and that of the annual cap are the same. However, it has been pointed out by *Leighton and Murray* [1966] that the increase of annual insolation with decreasing latitude will cause excess CO_2 ice to collect at the pole in a small residual cap. Recently, Mariner 9 photographs of the polar regions have disclosed residual caps with radii of the order of 2×10^2 km, compared to the 10^3-km annual caps. This furnishes an upper limit on the size of the perennial caps supplying and storing CO_2 ice. Using this value of a in (7) yields $\tau \approx 250$ yr. This is intermediate between the annual variations and the long-term variations in the obliquity of the order of a few times 10^4 yr implied by the frequencies $s_j' + \alpha \cos \Theta$ in (2). Hence the response to slow variations is considerably different from that to fast ones. Since $\tau^{-1} \gg s_j' + \alpha \cos \Theta$, (6) can be written

$$\Delta p \approx -\tfrac{1}{4}p_0 \frac{T^*}{T_0} \cot \Theta^* \cdot \sum_i N_i \sin [(s_i' + \alpha \cos \Theta)(t - \tau) + \gamma_i] \quad (8)$$

i.e., the pressure tracks the insolation variations with a phase lag of τ. Actually, the pressure variations are too large for the linearized solution to be of sufficient accuracy. Hence in practice it is best simply to neglect the phase lag and set

$$T = [(1 - A)\langle I_p \rangle / E\sigma]^{1/4} \quad (9)$$

equations (1) and (4) being used to compute p.

Figure 2 shows the resulting plots for the polar cap temperature and the mean atmospheric pressure for the past 5×10^6 yr resulting from this model. The periodicities reflect those of the obliquity: There are two dominant periods, 1.2×10^5 yr and 1.2×10^6 yr. The temperature ranges from ~130°K to ~160°K. When the obliquity is at its minimum of ~15°, most of the atmosphere freezes out at the poles and becomes incorporated into the residual caps while the pressure drops to a few tenths of a millibar. Our model is most accurate under these conditions, since atmospheric heat transport is undoubtedly negligible. When the obliquity is near its maximum of ~35°, the calculated atmospheric pressure approaches ~30 mbar. This is probably somewhat of an underestimate, since the model becomes less accurate at high pressures. Indeed it has been suggested [*Gierasch and Toon*, 1973; *Sagan et al.*, 1973; L. Yang, preprint, 1973] that a change in polar insolation could trigger an atmospheric feedback mechanism and drive the pressure to nearly 1 bar. At any rate, we can conclude that unless there is insufficient CO_2 on the planet, there have been periods in the recent history of Mars in which the

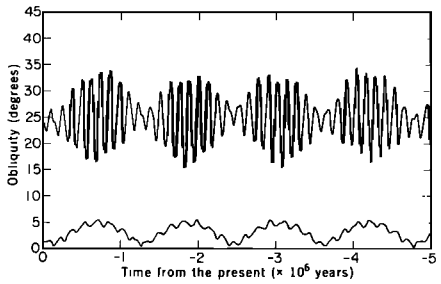

Fig. 1. Variations in the obliquity and orbital inclination of Mars for the past 5×10^6 yr [*Ward*, 1973].

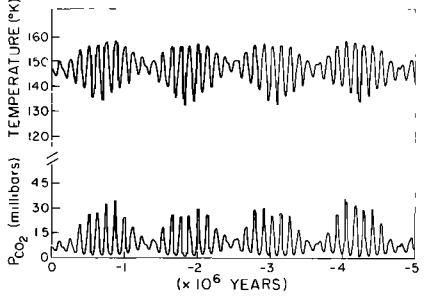

Fig. 2. Atmospheric pressure and polar cap temperature oscillations resulting from the obliquity variations for a Leighton-Murray equilibrium model with no atmospheric heat transport from equator to pole.

mass of the atmosphere was at least 4–5 times its present value.

The availability of CO_2 is somewhat of a problem. If our assumption that enough CO_2 is available is wrong, then the peaks of the pressure curves in Figure 2 must be truncated to reflect the proper upper limit. (It is the availability of volatiles that could limit the pressure. Carbon dioxide adsorbed in the regolith cannot be released unless very large pressures are first attained.) Strictly speaking, our inexact knowledge of such parameters as the albedo of CO_2 frost precludes even a definite conclusion in favor of the Leighton-Murray hypothesis of excess CO_2 ice for the present situation. However, the introduction of the obliquity oscillations lends fresh support to this proposal. The present mass of the atmosphere would represent an excess at times of low obliquity, and so at worst the Leighton-Murray model applies to these periods. At other times the obliquity is so great that a 6-mbar atmospheric pressure could not possibly be considered in equilibrium with the absorbed annual polar insolation. Hence we should have to be observing Mars at a very special time for the close agreement between pressure and polar insolation to exist in the absence of perennial CO_2 ice deposits.

If we grant the existence of excess CO_2, the next questions that come to mind are, How much material is there and where is it located? One possibility is that the observed residual caps are composed largely of CO_2 ice. However, there is a strong argument against the CO_2 composition of the south residual cap, first stated by *Murray and Malin* [1973], upon which we shall now elaborate.

Radio occultation measurements by *Kliore et al.* [1973] have indicated that the south polar region is at least 2 km higher in elevation than the north polar region. In deriving (3) (Appendix 1), the assumption was made that the temperatures of the north and south caps were equal. On the other hand, the barometric equation implies that

$$p_S/p_N = e^{-z/H} \tag{10}$$

where z is the polar height difference, H is the scale height, and p_S/p_N is the ratio of the polar pressures. When (10) is combined with the vapor pressure curve (4), there is an implied temperature difference ΔT:

$$z/H = T^*(T_S^{-1} - T_N^{-1}) \approx (T^*/T_0)(\Delta T/T_0) \tag{11}$$

For time scales longer than annual fluctuations, (9) is replaced by

$$2(1 - A)\langle I_p\rangle = E\sigma T_N^4 + E\sigma T_S^4 \tag{12}$$

indicating that the radiation losses from both poles are still equal to the total yearly polar insolation. From this it follows that $T_N \approx T_0 + \Delta T/2$ and $T_S \approx T_0 - \Delta T/2$, where T_0 is given by (9). Hence the north pole radiates more energy than its yearly insolation, and the south pole, less. To maintain equilibrium, a net amount of CO_2 is transferred from the south pole to the north pole with enough latent heat to restore the balance. From (A7) the net evaporation rate from the south pole averaged over a year is

$$dm/dt \approx (2E\sigma T_0^4/L)(\Delta T/T_0)$$
$$\approx 2[(1 - A)\langle I_p\rangle T_0/LT^*](z/H) \tag{13}$$

This rate is roughly 10 g/yr cm^2; i.e., a 100-m-thick perennial cap could be transferred from the south pole to the north pole in $\sim 2 \times 10^3$ yr. Since this time is short in comparison with the obliquity oscillation time scale, it is doubtful that a residual CO_2 ice cap would ever accumulate at the south pole.

If one is forced to relinquish the south pole as a possible site for perennial CO_2 ice deposits, then it is, needless to say, a rather uncomfortable premise that Mars has one water ice residual cap at the south pole and one CO_2 cap at the north pole. A possible solution is the suggestion by *Murray and Malin* [1973] that although most of the visible north residual cap is water, there exists also a large deposit of CO_2 ice. (Carbon dioxide cannot be buried under water ice, since the higher temperatures achieved by water ice during the summer will drive the CO_2 out.) They indicate a thick area in the north cap that is a likely candidate and estimate its mass to be of the order of 1–6 times that of the present atmosphere.

We close this section by pointing out that additional important information can be extracted from (6) if we replace $s_j' + \alpha \cos\Theta$ by $\tau'^{-1} \gg \tau^{-1}$. In this case, Δp becomes

$$\Delta p \approx \tfrac{1}{4}p_0 \frac{T^*}{T_0} \cot\Theta^*\left(\frac{\tau'}{\tau}\right) N \cos\left(\frac{t}{\tau'} + \gamma\right) \tag{14}$$

(for one forcing function with amplitude N). Note that the response is down by a factor of τ'/τ; i.e., the system is sluggish on time scales short in comparison with the characteristic time scale τ. One example of this is in the seasonal changes in the polar insolation considered in Appendix 1. However, the form of equation (14) is also applicable to short-term fluctuation in other parameters such as changes in the albedo. For a decrease in the albedo that persists for a year the increase in atmospheric pressure is only of the order of a percent of the value that one would calculate making the assumption that the system was always in equilibrium. In fact, it is fair to say that the system is in equilibrium with a time-averaged albedo, the average being taken over the time scale $\tau \approx 10^2$ yr and not necessarily with its instantaneous value. This complicates the interpretation of albedo and pressure measurements.

ANNUAL BEHAVIOR

Until now, effects with time scales much longer than the Martian year have been concentrated upon. However, it is also of interest to obtain some idea of the annual behavior of the CO_2 caps and the atmosphere at different epochs of the climatic history of Mars. A reasonable first approach to this problem is to perform a model calculation that attempts to isolate the influence of the insolation redistribution from other variables. We have calculated the condensation and evaporation of annual polar caps on a planet modeled as a smooth sphere with negligible heat conductivity and atmospheric heat transport. This calculation differs from that in Appendix 1 by including the dependence of the daily insolation on latitude. It is, of course, just this dependence that accounts for the advance and recession of the annual polar caps. Again it shall be assumed that there exists sufficient CO_2 to maintain a perennial ice cap at the north pole. The reader is cautioned at the outset, however, that this approach precludes an understanding of any coupling between changes in the insolation pattern and other phenomena such as atmospheric heat transport. We shall briefly return to this point later.

An analytic expression for the averaged daily insolation as a function of latitude δ can be derived [e.g., paper 1; *Cross*, 1971]:

$$\bar{I} = (S^*/\pi)\{\eta \sin\epsilon \sin\delta + \sin\eta \cos\epsilon \cos\delta\} \tag{15}$$

where

$$\cos \eta = -1 \qquad \delta > \pi/2 - \epsilon \text{ or } \delta < -\pi/2 - \epsilon$$
$$\cos \eta = -\tan \epsilon \tan \delta \qquad |\delta| < \pi/2 - |\epsilon| \qquad (16)$$
$$\cos \eta = +1 \qquad \delta < -\pi/2 + \epsilon \text{ or } \delta > \pi/2 + \epsilon$$

$$S^* = S(1 + e \cos v)^2/(1 - e^2)^2 \qquad (17)$$

$$\sin \epsilon = \sin \theta \sin (v + \omega) \qquad (18)$$

In the above expressions, v is the true anomaly of Mars, ω is the argument of perihelion measured from the vernal equinox of Mars, and ϵ is the latitude of the sun. In paper 1, daily insolation curves at various latitudes throughout the course of the Martian year are presented for the values $e = 0$, $\theta = 15°$, 25°, and 35°. These examples will be treated here. A copy of paper 1 is therefore useful for the following discussion.

The temperature of CO_2 frost is determined by the atmospheric pressure through the vapor pressure curve (4). Whenever the daily radiative losses at that temperature exceed the daily absorbed insolation at a given latitude, net condensation occurs, released latent heat maintaining the frost temperature. The rate of condensation per unit area is

$$dm/dt = [(1 - A)\bar{I} - E\sigma T^4]/L \qquad (19)$$

If one assumes that T varies little from the annual average (9) (this is equivalent to the approximation $\lambda \to \infty$ in Appendix 1), many features of the annual polar caps can be anticipated by looking at the shapes of the insolation curves in paper 1. The radiation losses being approximated by a horizontal line at the value $\langle I_p \rangle / S = (\sin \theta)/\pi(1 - e^2)^{1/2}$, the moment that condensation begins at a given latitude is determined by the intersection of this line with the appropriate descending portion of the insolation curve; i.e., the advance of the edge of the cap can be obtained from the relation $\bar{I} \approx \langle I_p \rangle$ [*Cross*, 1971]. The subsequent intersection during the rising portion of the insolation curve indicates when evaporation begins. It is clear from the insolation curves for present day ($e = 0.9$, $\theta = 25°$) shown in paper 1 that the south cap should extend to lower latitudes than the north cap. This is a property of the finite eccentricity and the current value of the argument of perihelion. This north-south asymmetry will oscillate as e and ω evolve, as is described in paper 1. It has been suggested (J. Briggs, preprint, 1973) that a large eccentricity and the resulting high insolation at the subsolar point may be involved in triggering global dust storms.

Equation (19) has been integrated numerically to obtain the mass per unit area m of the deposited frost as a function of time for various latitudes (Figures 3*a*–3*c*). By observing when m vanishes, the recession rate of the cap boundary can be acquired. Figure 4 shows the computed advance and recession for the three values of the obliquity. (Since a circular orbit is used, the north and south caps are symmetrical, and only one cap is shown.) The sensitivity of the system to changes in the obliquity is quite impressive. As the obliquity oscillates, so do the temperatures and the radiation losses from CO_2 frost anywhere on the planet. At the same time, since the total planet-wide insolation is not altered by an obliquity change, a warming of the summer pole implies a cooling of the winter pole. As a result, the computed maximum radius of the annual caps increases by nearly 20° for each 10° increment in the obliquity. In addition, the total CO_2 ice deposited shows a similar trend reaching ~110, ~180, and ~240 g/cm² at the pole for the three situations. The total mass of the annual caps

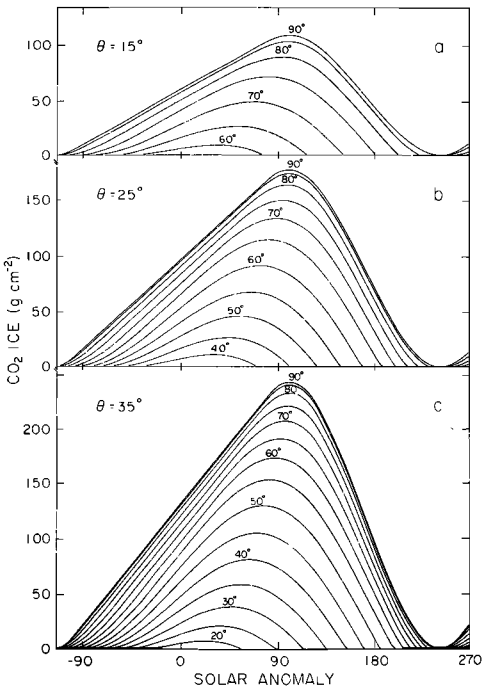

Fig. 3. CO_2 ice deposition of model annual caps for various latitudes during the year. Winter solstice is at zero solar anomaly.

can be found from integrating $m(\delta, t)$ over the appropriate hemisphere:

$$M(t) = 2\pi R^2 \int_0^{\pi/2} m(\delta, t) \cos \delta \, d\delta \qquad (20)$$

In addition, knowing the masses of the north and south caps as a function of time enables one to compute the fluctuations in the atmospheric presure:

$$\delta p \approx [g/4\pi R^2][M_N + M_S - \langle M_N + M_S \rangle] \qquad (21)$$

Figure 5 shows the integrated mass of the caps and the corresponding atmospheric pressure fluctuations. While the magnitude of δp increases with θ, the fractional variation $\delta p/p$ decreases with increasing obliquity. However, it should be realized that in maintaining the frost radiation temperature at a constant value in integrating (19), we have overestimated the pressure fluctuations. In reality, the frost temperature oscillates slightly with the pressure variations, this oscillation producing a damping effect. This effect is more important for a nonzero eccentricity (Appendix 1).

These calculations indicate that an increase in the obliquity

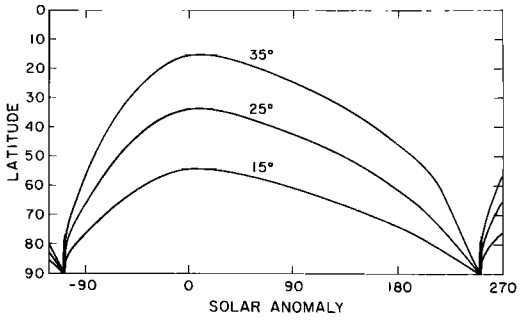

Fig. 4. Model calculations of annual cap boundary for obliquities of 15°, 25°, and 35°. Model treats only latitudinal redistribution of solar insolation.

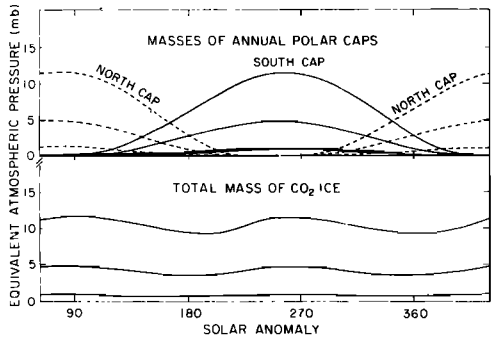

Fig. 5. (Top) Masses of the model caps in equivalent atmospheric pressure as a function of time. (Bottom) Total mass of CO_2 ice incorporated into both caps. Variation causes annual atmospheric pressure fluctuations.

and a heating of the polar region on an annual average cause the polar caps to enlarge greatly in both maximum coverage and total mass. It should be emphasized that in performing these calculations, the supply of CO_2 was always assumed to be adequate. From Figure 5 it is clear that an adequate supply requires not only enough to provide the equilibrium atmospheric pressure but a further excess to make up the annual caps. The mass of the annual caps is equivalent to ~1, ~5, and ~12 mbar for obliquity values of 15°, 25°, and 35°, respectively.

Discussion

Of the simplifications made in the preliminary calculations presented here the most serious omission is probably the neglect of atmospheric heat transport. Indeed the use of $A \approx 0.70$ as a model albedo may be taken as evidence for an appreciable atmospheric contribution to the polar heat balance, since the albedo of CO_2 frost is characteristically somewhat higher, i.e., ~0.75. However, the situation is not clear-cut because the model albedo refers to a time-averaged value that will undoubtedly be somewhat lower than the albedo of pure frost, owing to frequent contamination by low-albedo material.

The nature of the influence of atmospheric heat transport on the long-term behavior of the climate can be illustrated by determining the effect of the term

$$\beta(gH^2/\Omega R^2)p(1 - T/T_a)^2 \qquad (22)$$

inside the second set of brackets of (3). This is a rough order of magnitude estimate of the heat flux from equator to pole via baroclinic instability (Appendix 2). The air temperature $T_a \approx 200°K$ and $\Omega = 7 \times 10^{-4}$ s^{-1} is the spin angular velocity of Mars. The quantity β is a dimensionless factor of the order of unity but whose exact value is unknown. The linearized version of the equation for pressure variations now admits a solution of the form of (8) multiplied by (τ''/τ), where τ'' is the new characteristic response time given by

$$\frac{1}{\tau''} = \left(\frac{2agE\sigma T_0^5}{\pi R^2 L p_0 T^*}\right)\left[1 - \frac{\beta}{4}\left(\frac{p_0}{p^*}\right)\left(\frac{T_a}{T_0}\right)^4 \cdot\left(1 - \frac{T_0}{T_a}\right)\left(\frac{T^*}{T_0} - \frac{T^*}{T_a} - 2\frac{T_0}{T_a}\right)\right] \qquad (23)$$

with $p^* = E\sigma T_a^4\Omega R^2/gH^2 \approx 16.4$ mbar. (It is assumed that $\tau''^{-1} \gg s_j' + \alpha \cos\Theta$. The increments Δp and ΔT are measured with respect to p_0 and T_0, which satisfy $\mathfrak{IC}(\Theta^*) = 0$, where $\mathfrak{IC}$ is the net heat deposited at the pole, i.e., (B1). These are, of course, very close to the present values of p and T.) Whether increasing the role played by the atmosphere in maintaining the present heat balance increases or decreases the sensitivity of the system to insolation changes depends on the temperature T_0. (There is a low-temperature regime in which the atmospheric feedback of a greater pressure enhances the response to an increase in the polar insolation. This effect is more pronounced for a greater β. On the other hand, there is a high-temperature regime (with T not too different from T_a) in which an increase in $\langle I_p \rangle$ is opposed by a decrease in atmospheric heat transport caused by a drop in the temperature differential between the equator and the pole. In this case, variations in the polar temperature and pressure are less for larger β.)

Combining (7), (23), and (B1), one finds that $d(\tau''/\tau)/d\beta > 0$ if

$$T_0/T_a < 1 + \tfrac{1}{4}(T^*/T_a) - \tfrac{1}{2}[\tfrac{1}{4}(T^*/T_a)^2 + 4]^{1/2} \qquad (24)$$

For the values used here the condition reads $T_0 < 175°K$, so that we underestimate the response by setting $\beta = 0$. The linear solution is not accurate even for zero atmospheric heat transport. By neglecting the phase lag, the pressure oscillations are most accurately calculated by setting $\mathfrak{IC} = 0$. Since we have no reliable handle on the value of β, we shall not present pressure curves for nonzero values. However, certain characteristics of the system can still be described. For example, if β is too large, τ'' is negative, and the linear solution contains an exponentially growing term. In this case the atmosphere–polar cap equilibrium is unstable, and the polar CO_2 deposits will evaporate and try to establish a new equilibrium state at a higher pressure. The possibility of an instability of this type was first proposed by *Sagan et al.* [1973] and has been discussed in detail by *Gierasch and Toon* [1973]. There is therefore a limit to how large the present atmospheric contribution to the polar heat balance can be and still be consistent with the existence of perennial CO_2 ice deposits. For the model used here this value of β is ~2.97, which corresponds to a contribution of ~25.7% of the energy radiated away from a permanent CO_2 cap in equilibrium with the 6-mbar atmosphere. (This is found by setting $\tau''^{-1} = 0$. This is in fair agreement with the paper by *Gierasch and Toon* [1973]. From their Figure 2*b*, one can roughly estimate ~21% as the critical atmospheric contribution at which 6 mbar is unstable.)

The instability above has been suggested as a means of producing a transition between high- and low-pressure states in the climatic history of Mars [*Sagan et al.*, 1973]. There is a possibility that such a high-pressure state could not be released once it is established. This would, of course, contradict the present situation. We have investigated the condition under which release is possible when the obliquity decreases to 15° for the simplified model treated here (Appendix 2) and have found that release can be achieved provided $\beta \leq 2.77$. This value is equivalent to a present atmospheric contribution of ~23.8%. Another possibility is that the atmosphere becomes CO_2-limited before a high-pressure equilibrium state is attained. (For the estimate of CO_2 ice given by *Murray and Malin* [1973] the peak pressures would still be of the same order of magnitude as those shown in Figure 2.) This discussion has pertained to a pure CO_2 perennial cap. Gierasch and Toon point out, however, that if the polar caps are composed of a CO_2 hydrate, as is suggested by *Miller and Smythe* [1970], the system is stabilized, because the vapor pressure curve is not as steep.

Our calculations of the annual caps could also be significantly altered by including atmospheric heat transport. The calculations of the conditions during high obliquity are the most subject to change. However, the nature of this modification is not always apparent. For example, the atmosphere warms the winter hemisphere at the expense of the summer hemisphere and would tend to inhibit frost deposition and decrease the maximum coverage of the annual cap. On the other hand, if the atmospheric feedback drove the pressure considerably higher at periods of larger obliquity than that used in our calculation, CO_2 frost would condense at a higher temperature via the vapor pressure curve. This result would tend to increase the coverage of the annual cap. Numerical models of the annual caps including atmospheric transport for past climatic conditions are needed to settle such questions.

The effects of pressure variations on the physical environment are, of course, of extreme interest. As an example, we close this section with a brief rediscussion of the eolian erosion models of *Ryan* [1964] and *Sagan and Pollack* [1967, 1969]. Of particular interest is the dependence of these models on the atmospheric density ρ, which shall be assumed to vary by an order of magnitude above and below the current value.

Let V_0 be the horizontal wind velocity. The main streamflow is separated from the surface by the Eckman layer with a thickness of the order of $\delta \approx (\nu/\Omega)^{1/2}$, where ν is the effective kinematic viscosity. If the flow in the boundary layer is laminar, $\nu = \eta/\rho$, where $\eta \approx 1.5 \times 10^{-4}$ g/cm s is the dynamic viscosity of the Martian atmosphere [*Ryan*, 1964]. If $\rho \approx 1 \times 10^{-5}$ g/cm^3 for a 6-mbar atmosphere, $\delta \approx 1.6 \times 10^2$ cm. The Reynolds number for the laminar Eckman layer is $Re_{t,E} \approx V\delta/\nu \approx 1 \times 10^4 V_3$, where $V_3 = 10^{-3} \times V_0$ (cm/s). Typical thermal wind velocities are $V_0 \approx C^2(1 - T_p/T_a)/\Omega R \approx$ (few) $\times 10^3$ cm/s, so that the Reynolds number is of the order of a few times 10^4. The critical number for the onset of turbulent flow in the boundary layer is $Re^* \approx 5 \times 10^2$ [*Landau and Lifshitz*, 1959]. Since the laminar Reynolds number depends on $\rho^{1/2}$ through the boundary layer thickness and the kinematic viscosity, it appears that the boundary layer will be turbulent, even if the density drops an order of magnitude during periods of low obliquity. (Gravitational stratification is unimportant, since the Richardson number $Ri = (gd\rho/dz)/\rho(dv/dz)^2 \approx g\delta^2/V^2H \approx 10^{-6}$ is much less than the critical value of ¼ [i.e., *Chandrasekhar*, 1961].) In this case the boundary layer thickness is calculated by using the effective turbulent viscosity $\nu_t \approx \nu(Re_{t,E}/Re^*)$, where $Re_{t,E} \approx \delta_t V/\nu$ is the turbulent Eckman layer Reynolds number. Hence $\delta_t \approx V/\Omega Re^* \approx 2.8 \times 10^3 V_3$ cm. The turbulent boundary layer thickness depends only on the wind speed. On the other hand, large-scale winds such as thermal winds and winds produced by large-scale topography are relatively insensitive to density variations. (For example, the thermal wind velocity is influenced by the equator-pole temperature differential. However, this varies by only ~50% over the pressure range of Figure 2.) Hence we can expect δ_t to be typically of the order of $\sim 10^4$ cm, which is just the value employed by *Sagan and Pollack* [1967].

In the turbulent boundary layer the velocity profile is logarithmic [*Landau and Lifshitz*, 1959]:

$$V \approx 2.5 v_* \log_e (Z/k) \tag{25}$$

where Z is the vertical distance above the surface, k is a characteristic length, and v_* is an effective velocity related to the surface stress S by $S \approx \rho v_*^2$. *Sagan and Pollack* [1969] use $k \approx a'/5$ for rough surfaces and $k \approx a'/15$ for smooth surfaces, where a' is an effective grain radius. However, if the surface is smooth, k is determined by the viscous sublayer $\sim \nu/v_*$ [*Landau and Lifshitz*, 1959]. For the values that we are interested in, $\nu/v_* \approx 400$ μm. In view of the logarithmic dependence of (25), this modification should be minor. The free stream velocity V_0 is obtained from (25) with $Z = \delta_t$.

The threshold velocity for grain movement is given by

$$v_{*,t} = A(2ag\rho_p/\rho)^{1/2} \tag{26}$$

where a is the grain radius and ρ_p is the grain density. The value of A depends on the Reynolds number for the grains, defined as $Re_{gr} \approx 2av_*/\nu$. Sagan and Pollack find from the data of *Bagnold* [1941] that if $Re_{gr} \gtrsim 2$, $A \approx 10^{-1}$, whereas for $Re_{gr} \lesssim 2$, A increases with decreasing Reynolds number in such a way that $v_{*,t}$ goes through a minimum. We show in Appendix 3 that a consequence of the assumption that A depends only on the Reynolds number is that $(v_{*,t})_{\min} \propto \rho^{-2/3}$. In addition, the radius of the grains most easily moved a_T is proportional to $\rho^{-1/3}$. From (25), $(V_{0,t})_{\min}$ is also nearly proportional to $\rho^{-2/3}$ (neglecting variations in the Eckman layer thickness and the characteristic length k). Sagan and Pollack find $(v_{*,t})_{\min} \approx 3.5$ m/s, $a_T \approx 250$ μm, and $(V_{0,t})_{\min} \approx$ 100 m/s for a 5-mbar atmospheric pressure. If the density varies by 2 orders of magnitude, $(v_{*,t})_{\min}$ and $(V_{0,t})_{\min}$ vary by a factor of ~22 and a_T by a factor of ~5. Hence surface material should be much more frequently moved during periods of high atmospheric pressure. (In fact, Ryan's discussion of wind erosion is for pressures of 25 and 80 mbar.) During periods of low obliquity the required threshold velocity is $(V_{0,t})_{\min} \approx 500$ m/s, which considerably exceeds the sound speed. Even if such winds could be generated, their energy would quickly be dissipated by shocks. Hence eolian erosion should be virtually absent during the lowest obliquity. Also although the most easily moved grain a_T is smaller for larger density, for a given V_0 a wider range of grain sizes can be moved. In particular, the radius of the largest saltating particle $a_{\max}$ is proportional to $\rho^{1/2}$.

These considerations indicate that pressure fluctuations are extremely important to the mechanism of eolian erosion. Low-pressure intervals are quiescent periods, whereas high-pressure intervals may be characterized by frequent and severe dust storms.

CONCLUSION

Oscillations in the obliquity of Mars produce large changes in the climate provided the atmosphere exists in equilibrium with perennial CO_2 ice deposits at the north pole, as was originally suggested by *Leighton and Murray* [1966]. An atmospheric pressure of 6 mbar at the present obliquity of 25° drops to ~0.3 mbar when the obliquity is at its minimum of 15° and rises to at least ~30 mbar when the obliquity is at its maximum of 35°. The temperature of CO_2 ice varies from ~130° to ~160°K between these extremes. The peak pressure can be higher if atmospheric heat transport from the equator to the pole is significant. The characteristic response time of the system is of the order of ~250 yr. Although the system closely follows the obliquity changes that occur on a time scale of a few times 10^4 yr, it is stable against short-term insolation changes. The 2-km-higher elevation of the south polar region over the north polar region reported by *Kliore et al.* [1973] implies that the south residual cap is water ice, since CO_2 ice would migrate to the north pole at a rate of ~10 g/cm^2 yr. Model calculations indicate that the heating of the polar regions on an annual basis by increasing the obliquity

may cause the annual caps to enlarge in both mass and maximum coverage. Finally, the mechanism of eolian erosion is intensified by an increase in atmospheric pressure. The minimum threshold velocity for grain movement is proportional to $\rho^{-2/3}$, which varies by a factor of ~22 over the pressure range described. Many other issues, such as the stability of liquid water, also deserve investigation, although we have not attempted to investigate them here. At any rate, it appears quite probable that the climate of Mars experiences periodic modifications of substantial strength, and there is considerable motivation to try to relate this phenomenon to the many unusual surface features on the planet.

APPENDIX 1

Perhaps the simplest model illustrating the essentials of the control of a CO_2 atmosphere by perennial ice deposits at the poles is the following. Consider two blocks of CO_2 ice, each with area a in a container of volume $V = 4\pi R_m^2 H$, where R_m is the radius of Mars and H is the scale height of the atmosphere. Let this container also hold CO_2 gas at a pressure p. The blocks, representing the north and south poles, are irradiated alternately by a solar flux of the form

$$I = \langle I_p \rangle \mathfrak{F}(e, v, \omega) \tag{A1}$$

where $\mathfrak{F}$ is chosen as being appropriate for the poles, v is the true anomaly, ω is the argument of perihelion, and $\langle I_p \rangle$ is the annual polar average given by (1). Hence we are neglecting latitudinal differences in the insolation; i.e., the polar regions are treated as being 'flat.'

The basic equations governing the evolution of this system are the following.

Equation of heat balance

$$\rho C h\, dT/dt = (1 - A)I - E\sigma T^4 - L\, dm/dt \tag{A2}$$

where ρ, C, h, and T are the density, specific heat capacity, depth, and temperature of the CO_2 ice (there are two such equations, one for each pole). This equates the rate of change of the energy content of the ice to the difference between the power received by solar insolation and that lost by radiation and evaporation of CO_2 frost. (We have ignored the finite time for heat diffusion, so that the heat capacity of the CO_2 ice in (A2) is an upper limit.)

Vapor pressure curve for CO_2 ice

$$p_v = Be^{-T^*/T} \tag{A3}$$

Equation approximating evaporation rate in terms of disequilibrium between CO_2 ice and atmospheric pressure

$$dm/dt \approx (p_v - p)/c \tag{A4}$$

where c is the gas sound speed.

Equation relating change in atmospheric pressure to evaporation at both poles (conservation of mass)

$$dp/dt = [ag/4\pi R_m^2][dm_n/dt + dm_s/dt] \tag{A5}$$

where g is the surface acceleration of gravity. We employ $\rho \approx 1.5$ g/cm^3 and $C \approx 0.9 \times 10^7$ erg/g °K. Numerical values for the other constants in (A2)–(A5) can be found in the main text.

The physical properties of CO_2 ice, especially its very high vapor pressure, allow several simplifications to be made. If the cap were seriously out of equilibrium with the atmosphere, (A4) would imply that the last term of (A2) would be $O[Lp_v/c] \approx 5 \times 10^7$ erg/cm^2 s, compared to $O[(1 - A)I] \approx 2 \times 10^4$ erg/cm^2 s. Hence the surface temperature of the cap is dominated by very strong evaporative cooling, which quickly establishes $p_v \approx p$. It is also true that for cases of interest here,

$$\frac{\rho C h\, dT/dt}{L\, dm/dt} \approx \frac{\rho C a g h T^2}{4\pi R_m^2 L p T^*} \ll 1 \tag{A6}$$

i.e., the heat capacity of the cap is relatively unimportant. Therefore (A2) can be written

$$dm/dt \approx L^{-1}[(1 - A)I - E\sigma T^4] \tag{A7}$$

Combining (A1), (A5), and (A7) yields

$$dp/dt \approx [ag/2\pi R_m^2 L][\tfrac{1}{2}(1 - A)\langle I_p \rangle(\mathfrak{F}_n + \mathfrak{F}_s) - E\sigma T^4] \tag{A8}$$

Physical intuition suggests that the pressure variation be divided into two parts, $p = p' + \delta p$, where δp represents annual pressure fluctuations that result from the time variation of $(\mathfrak{F}_n + \mathfrak{F}_s)$ and p' represents longer-term adjustments, which would still occur in the absence of annual variations. Let p' be the solution of

$$dp'/dt = [ag/2\pi R_m^2 L][(1 - A)\langle I_p \rangle - E\sigma T'^4] \tag{A9}$$

By utilizing this equation, it is easy to show that T' and p' decay to the values

$$T_0 = [(1 - A)\langle I_p \rangle / E\sigma]^{1/4} \qquad p_0 = Be^{-T^*/T_0} \tag{A10}$$

in a time scale of the order of

$$\tau \approx \pi R_m^2 L p_0 T^*/2agT_0(1 - A)\langle I_p \rangle \tag{A11}$$

This is the basic tenet of the Leighton-Murray model.

To compute the annual fluctuations δp, subtract (A9) from (A8), linearize the terms containing $T = T' + \delta T$, and eliminate δT by using a linearized version of (A3):

$$d\delta p/dt + \delta p/\lambda\tau \approx \frac{1}{4}\frac{p_0}{\tau}\left(\frac{T^*}{T_0}\right)[\tfrac{1}{2}(\mathfrak{F}_n + \mathfrak{F}_s) - 1] \tag{A12}$$

The function $\frac{1}{2}(\mathfrak{F}_n + \mathfrak{F}_s)$ can be determined from (15)–(18) with $\delta = \pm\pi/2$:

$$\tfrac{1}{2}(\mathfrak{F}_n + \mathfrak{F}_s) = (\pi/2)(1 - e^2)^{-3/2} \cdot (1 + e\cos v)^2 |\sin(v + \omega)| \tag{A13}$$

We have 'tagged' the time constant τ on the left side of (A12) to facilitate the later taking of a limit. In general, that term has a relatively minor damping effect. Physically, it arises from small changes in the radiation loss rate as the cap temperature fluctuates with the pressure. If it is neglected ($\lambda \to \infty$), (A12) can be integrated directly. During the northern summer $0 < v - \omega < \pi$,

$$\delta p_n = \frac{p_0}{4n\tau}\left(\frac{T^*}{T_0}\right)\left[C_n - nt - \frac{\pi}{2}\cos(v + \omega)\right] \tag{A14}$$

whereas during the southern summer $\pi < v - \omega < 2\pi$,

$$\delta p_s = \frac{p_0}{4n\tau}\left(\frac{T^*}{T_0}\right)\left[C_s - nt + \frac{\pi}{2}\cos(v + \omega)\right] \tag{A15}$$

Matching these two equations at the equinoxes yields only

one condition for the constants, $C_s - C_n = \pi$. We can remove this indeterminacy by requiring $\oint \delta p\, dt = 0$. For $e = 0$, $nt = v$, and $\omega = 0$ the constants are

$$C_n = \pi/2 \qquad C_s = 3\pi/2 \tag{A16}$$

The minimum and maximum occur at $\sin^{-1}(2/\pi) \equiv \sim 40°$ and $\pi - \sin^{-1}(2/\pi) \equiv \sim 140°$, respectively, during the northern summer and at $\sim 220°$ and $\sim 320°$ during the southern summer. The total excursion in the pressure is

$$\max \delta p - \min \delta p = \frac{p_0}{4n\tau}\left(\frac{T^*}{T_0}\right)(2 \sin^{-1}(2/\pi) - \pi + \pi \cdot [1 - (2/\pi)^2]^{1/2}) \tag{A17}$$

which yields a value of the order of

$$0.68(p_0/4n\tau)(T^*/T_0)$$

A solution of (A12) including the damping term is not difficult to obtain. The solution for zero eccentricity can be written as

$$\delta p_{n(s)} = \frac{p_0}{4n\tau}\left(\frac{T^*}{T_0}\right)\left\{C_{n(s)}e^{-t/\lambda\tau} - \lambda n\tau(1 - e^{-t/\lambda\tau}) (\mp)\frac{\pi}{2}[1 + (\lambda n\tau)^{-2}]^{-1}[\cos nt - (\lambda n\tau)^{-1}\sin nt]\right\} \tag{A18}$$

with $\lambda = 1$. The damping term removes the indeterminacy, and the constants are uniquely given as

$$\begin{aligned} C_n &= -\lambda n\tau + \pi[1 + (\lambda n\tau)^{-2}]^{-1}(1 - e^{-\pi/\lambda\tau})^{-1} \\ C_s &= -\lambda n\tau + e^{\pi/\lambda\tau n}\pi[1 + (\lambda n\tau)^{-2}]^{-1}(1 - e^{-\pi/\lambda\tau})^{-1} \end{aligned} \tag{A19}$$

We invite the reader to take the limit $\lambda \to \infty$ of the above expressions and show that (A19) reduces to (A16) and (A18) yields (A14) and (A15) with $e = 0$, $\omega = 0$, and $nt = v$.

The effect of a finite eccentricity can be appreciated by using (A14) and (A15), which can be written

$$\delta p_{n(s)} = \frac{p_0}{4n\tau}\left(\frac{T^*}{T_0}\right) \cdot \left[C_{n(s)} - v - 2e \sin v\,(\mp)\frac{\pi}{2}\cos(v + \omega)\right] \tag{A20}$$

to first order in e. The positions of the minimums and maximums are given by

$$(\pm)\sin(v + \omega) = (2/\pi)(1 - 2e \cos v) \tag{A21}$$

These are displaced from their positions v_0 for $e = 0$ by

$$\delta v \approx (\mp)\frac{4e}{\pi}\frac{\cos v_0}{\cos(v_0 + \omega)} \tag{A22}$$

which has a maximum value of about 8.5° for $e = 0.09$.

We have also obtained a solution to first order in e including the damping term in (A12). However, the result is somewhat cumbersome, and we shall not reproduce it here.

Appendix 2

The rationale behind choosing the functional form (22) is as follows. The heat flux over the pole is of the order of $\sim \rho VRHc^2(1 - T/T_a)$, where ρ is the air density, V is the wind velocity from lower latitudes toward the poles, c is the sound speed, and T_a is the air temperature. If the poleward flux is due principally to baroclinic instability, the velocity is of the order of $V \approx c^2(1 - T/T_a)/\Omega R$, where Ω is the spin velocity of Mars. Combining these expressions and dividing the heat flux by the area of the polar region $\sim R^2$ yields the desired functional form. We also found it to be convenient to express the result in terms of the scale height $H \approx c^2/g \approx 10$ km and the pressure $p \approx \rho c^2$. This is a rough order of magnitude estimate at best. Atmospheric heat transport is strongly seasonally dependent and must be averaged over a year. Quantities such as the poleward wind velocity can only be approximated. A dimensionless constant β, which is essentially the ratio of the actual heat transport to that given by the dimensional analysis, has been included.

The net power deposited at the poles is given by

$$\mathfrak{IC} = (1 - A)\langle I_p\rangle + \beta(gH^2/\Omega R^2)p(1 - T/T_a)^2 - E\sigma T^4 \tag{B1}$$

In general, (for interesting values of β) this expression goes first through a minimum and then through a maximum as T/T_a runs from 0 to 1. These extremums are located by setting the derivative

$$d\mathfrak{IC}/dT = \beta(gH^2/\Omega R^2)(p/T)(1 - T/T_a) \cdot [T^*/T - T^*/T_a - 2(T/T_a)] - 4E\sigma T^3 \tag{B2}$$

equal to zero. An equilibrium state ($\mathfrak{IC} = 0$) is stable if $d\mathfrak{IC}/dT < 0$. Thus there are no stable states between the temperatures of minimum and maximum $\mathfrak{IC}$. A low-pressure state evolves to a high-pressure one if $\langle I_p\rangle$ becomes so large that $\mathfrak{IC}_{\min} > 0$, whereas a transition form high- to low-pressure occurs if $\langle I_p\rangle$ becomes so small that $\mathfrak{IC}_{\max} < 0$. In both cases the condition for marginal stability is $\mathfrak{IC} = d\mathfrak{IC}/dT = 0$. Equations (B1) and (B2) can be nondimensionalized by the substitutions $T' = T/T_a$, $I' = (1 - A)\langle I_p\rangle/E\sigma T_a^4$, $p' = p/p^*$, $T'^* = T^*/T_a$,

$$I' + \beta p'(1 - T')^2 - T'^4 = 0 \tag{B3}$$

and

$$\beta p'(1 - T')[T'^*(1 - T') - 2T'^2] - 4T'^5 = 0 \tag{B4}$$

Eliminating $\beta p'$ yields

$$F(T') = (T'^4 - I')\{T'^*(1 - T') - 2T'^2\} - 4T'^5(1 - T') = 0 \tag{B5}$$

The function $F(T')$ has been plotted by using the values $T'^* = 15.740$ and $I' = 0.1836$, corresponding to $\theta = 15°$. The intersection of the descending portion of the line with the zero axis yields the value $T' = 0.860$ or $T = 172°$K. Substitution of this into (B3) yields

$$\beta = (T'^4 - I')/p'(1 - T')^2 \tag{B6}$$

which, together with the vapor pressure curve, gives the upper limit $\beta < 2.50$. This corresponds to 21.7% of the present polar heat balance. The value of I' should be corrected to $I' = 0.1438$. A second calculation yields $\beta < 2.77$.

Appendix 3

The threshold velocity is obtained from the equation

$$v_{*,t} = A(2ag\rho_p/\rho)^{1/2} \tag{C1}$$

where A is nearly constant and equal to $\sim 10^{-1}$ provided the Reynolds number

$$Re = 2av_*/\nu \tag{C2}$$

is above some critical value Re'. Past this point, A increases with decreasing Re. *Ryan* [1964] states $Re' \approx 3.5$, whereas *Sagan and Pollack* [1967] prefer $Re' \approx 2$.

Sagan and Pollack claim that a plot of $v_{*,t}$ versus a for a given ρ goes through a minimum very near Re', so that A is still constant. Equations (C1) and (C2) can be combined to yield $(v_{*,t})_{\min} \propto \rho^{-2/3}$ and $a_T \propto \rho^{-1/3}$. However, both their plots of $v_{*,t}$ and those of Ryan's indicate that $(v_{*,t})_{\min}$ occurs closer to $Re' \approx 1$. Nevertheless, the same density dependence of the minimum threshold velocity is still valid provided the weaker assumption is made that A depends only on the Reynolds number. Squaring (C1) and differentiating yield

$$(\partial v_*/\partial a)_\rho = (v_*/a) \cdot [A^2 + (2av_*/\nu)\, dA^2/dRe]/[\rho v_*^2/\rho_p a g - (2av_*/\nu)\, dA^2/dRe] \quad \text{(C3)}$$

The minimum requires $(\partial v_*/\partial a)_\rho = 0$, which implies

$$(dA^2/dRe)_{Re_{crit}} = -A^2(\nu/2av_*) = -A^2/Re_{crit} \quad \text{(C4)}$$

Equation (C4) depends only on the Reynolds number. Hence its solution, Re_{crit}, which gives the Reynolds number at which the threshold velocity curve goes through a minimum, is density independent. In addition, the value of $A(Re_{crit}) = A_{crit}$ at $(v_{*,t})_{\min}$ is density independent. It follows that (C1) and (C2) evaluated at the minimum can indeed be combined to yield

$$(v_{*,t})_{\min} = [g\rho_p \eta Re_{crit} A_{crit}^2]^{1/3} \rho^{-2/3} \quad \text{(C5)}$$

$$a_T = (\eta^2/2g\rho_p)^{1/3} (Re_{crit} A_{crit})^{2/3} \rho^{-1/3} \quad \text{(C6)}$$

However, this density dependence is not a consequence of constant behavior of A for Reynolds numbers greater than Re' nor of a coincidence of $(v_{*,t})_{\min}$ with Re'.

Acknowledgments. This research was supported by NASA grant NGR 05-002-117 at the California Institute of Technology. This paper was presented at the International Colloquium on Mars, Jet Propulsion Laboratory, California Institute of Technology, Pasadena, California 91109, November 28 to December 1, 1973. Contribution 2368 of the Division of Geological and Planetary Sciences, California Institute of Technology.

REFERENCES

Bagnold, R. A., *The Physics of Blown Sand and Desert Dunes*, Methuen, London, 1941.

Blasius, K. R., A study of Martian topography by analytic photogrammetry, *J. Geophys. Res., 78,* 4411, 1973.

Blumsack, S. L., On the effects of large-scale temperature advection in the Martian atmosphere, *Icarus, 15,* 429, 1971.

Chandrasekhar, S., *Hydrodynamic and Hydromagnetic Stability*, Oxford University Press, New York, 1961.

Cross, C. A., The heat balance of the Martian polar caps, *Icarus, 15,* 110, 1971.

Cuzzi, J. N., and D. O. Muhleman, The microwave spectrum and nature of the subsurface of Mars, *Icarus, 17,* 548, 1972.

Fanale, F. P., and W. A. Cannon, Adsorption on the Martian regolith, *Nature, 230,* 502, 1971.

Gierasch, P. J., and C. Sagan, A preliminary assessment of Martian wind regimes, *Icarus, 14,* 312, 1971.

Gierasch, P. J., and O. B. Toon, Atmospheric pressure variations and the climate of Mars, *J. Atmos. Sci., 30,* 1502, 1973.

Kliore, A. J., G. Fjeldbo, B. L. Seidel, M. J. Sykes, and P. M. Woiceshyn, *S* band radio occultation measurements of the atmosphere and topography of Mars with Mariner 9: Extended mission coverage of polar and intermediate latitudes, *J. Geophys. Res., 78,* 4331, 1973.

Landau, L. D., and E. M. Lifshitz, *Fluid Mechanics*, pp. 145–167, Addison-Wesley, Reading, Mass., 1959.

Leighton, R. B., and B. C. Murray, Behavior of carbon dioxide and other volatiles on Mars, *Science, 153,* 136, 1966.

Leovy, C., and Y. Mintz, Numerical simulation of the atmosphere circulation and climate of Mars, *J. Atmos. Res., 26,* 1167, 1969.

McCauley, J. F., M. H. Carr, J. A. Cutts, W. K. Hartmann, H. Masursky, D. J. Milton, R. P. Sharp, and D. E. Wilhelms, Preliminary Mariner 9 report on the geology of Mars, *Icarus, 17,* 289, 1972.

Miller, S. L., and W. D. Smythe, Carbon dioxide clathrate in the Martian ice cap, *Science, 170,* 531, 1970.

Murray, B. C., and M. C. Malin, Polar volatiles of Mars—Theory versus observation, *Science, 182,* 437, 1973.

Murray, B. C., A. Soderblom, J. A. Cutts, R. P. Sharp, D. J. Milton, and R. B. Leighton, Geological framework of the south polar region of Mars, *Icarus, 17,* 328, 1972.

Murray, B. C., W. R. Ward, S. C. Yeung, Periodic insolation variations on Mars, *Science, 180,* 638, 1973.

Ryan, J. A., Notes on the Martian yellow clouds, *J. Geophys. Res., 69,* 3759, 1964.

Sagan, C., and J. B. Pollack, A windblown dust model of Martian surface features and seasonal changes, *Spec. Rep. 255,* Smithson. Astrophys. Observ., Cambridge, Mass., 1967.

Sagan, C., and J. B. Pollack, Windblown dust on Mars, *Nature, 223,* 791, 1969.

Sagan, C., O. B. Toon, and P. J. Gierasch, Climatic change on Mars, *Science, 181,* 1045, 1973.

Soderblom, L. A., M. C. Malin, J. A. Cutts, and B. C. Murray, Mariner 9 observations of the surface of Mars in the north polar region, *J. Geophys. Res., 78,* 4197, 1973.

Ward, W. R., Large-scale variations in the obliquity of Mars, *Science, 181,* 260, 1973.

Ward, W. R., Climatic variations on Mars, 1, Astronomical theory of insolation, *J. Geophys. Res.*, this issue, 1974.

Washburn, E. W. (Ed.), *International Critical Tables of Numerical Data, Physics, Chemistry, and Technology*, vol. 3, McGraw-Hill, New York, 1948.

(Received February 5, 1974;
revised April 8, 1974.)